PENSOFT
SENCKENBERG world of biodiversity
Leibniz Association

Intraspecific structure of *Myotis petax* Hollister, 1912 (Chiroptera: Vespertilionidae) based on mitochondrial DNA and morphological data

Uliana V. Gorobeyko[1], Denis V. Kazakov[2,3], Anastasia A. Kadetova[4], Irina N. Sheremetyeva[1], Valentin Yu. Guskov[1], Irina V. Kartavtseva[1], Nikolai E. Dokuchaev[5], Evgeniy S. Zakharov[6], Sergei V. Kruskop[7]

1 *Federal Scientific Center of the East Asia Terrestrial Biodiversity, Far Eastern Branch of the Russian Academy of Sciences, 100-let Vladivostoka, 159, 690022 Vladivostok, Russia*
2 *Institute of General and Experimental Biology, Siberian Branch of the Russian Academy of Sciences, Sakh'yanovoy, 6, 670047 Ulan-Ude, Russia*
3 *Institute of Environmental and Agricultural Biology (X-BIO), University of Tyumen, Volodarskogo, 6, 625003 Tyumen, Russia*
4 *Moscow Zoo, Bolshaya Gruzinskaya, 1, 123242 Moscow, Russia*
5 *Institute of Biological Problems of the North, Far Eastern Branch of the Russian Academy of Sciences, Portovaya, 18, 685000, Magadan, Russia*
6 *Institute of Natural Sciences, Ammosov North-Eastern Federal University, Yakutsk, Russia*
7 *Zoological Museum, Lomonosov Moscow State University, Bolshaya Nikitskaya, 2, 125009 Moscow, Russia*

https://zoobank.org/5E5C46AC-DD63-40F1-AA00-85FF4EA9B8DF

Corresponding author: Uliana V. Gorobeyko (ekz.bio@ya.ru)

Academic editor Clara Stefen | **Received** 14 August 2024 | **Accepted** 6 March 2025 | **Published** 21 March 2025

Citation: Gorobeyko UV, Kazakov DV, Kadetova AA, Sheremetyeva IN, Guskov VYu, Kartavtseva IV, Dokuchaev NE, Zakharov ES, Kruskop SV (2025) Intraspecific structure of *Myotis petax* Hollister, 1912 (Chiroptera: Vespertilionidae) based on mitochondrial DNA and morphological data. Vertebrate Zoology 75 87–106. https://doi.org/10.3897/vz.75.e134683

Abstract

Myotis petax is a common and widespread Asian bat species, whose intraspecific sequence variability remains poorly understood. In this work we analyzed the variability of the mitochondrial control region and craniometric measurements for an extensive sample set originating from the entire species range. This made it possible to identify the main genetic lineages and to compare their distribution with the morphological groups. From our investigations, we found that the prevalent genetic lineages, namely, "Siberia," "Amur," and "Okhotsk," appear to be connected to large river systems. The cohabitation of various genetic lineages occurs only in territories where different river basins are connected, such as the Primorsky Territory, Khabarovsk Territory, Transbaikalia Territory, and Mongolia. Moreover, we discovered that the five morphological groups (Siberia, Okhotsk, Amur, Kunashir, and Korea) are partially correlated with previously identified genetic lineages and subspecies. However, *M. p. petax* and *M. p. loukashkini* were the only two out of the five subspecies that could be well-defined using specific mtDNA sequences and morphological descriptions. Nonetheless, the subspecies *M. p. ussuriensis* does not have a distinct genetic lineage to allow for their classification. Notably, a specific mix of morphological group and a genetic lineage characterize the "Amurian morphological form," which may support its validity as a subspecies rank. That notwithstanding, more information is needed to fully unravel the intraspecific structure of *M. petax* in the southern Far East and potential contact zones of diverse forms.

Keywords

Bat, control region, craniometric variability, Far East, genetic variability, Siberia

Introduction

The Eastern water bat, *Myotis petax* Hollister, 1912, is a common and widespread Asian bat species. It prefers near-water habitats and often forages at a height of less than 10 cm above the water surface (Tiunov 1997). *Myotis petax* is considered a sedentary species that spends the winter in caves or mines. However, there is a noticeable discrepancy between the species' summer and winter abundance in the Russian Far East. It has also been observed that some individuals seem to prefer different kinds of hibernation sites while others migrate outside of summer habitat (Tiunov 1985). The species' range extends from Western Siberia to the Far East of Russia, Northeast China, Korea, and Japan, and in the south reaches Northern Mongolia (Botvinkin 2002; Smith et al. 2008; Bernikov et al. 2011; Zhigalin and Khritankov 2014; Kawai 2015; Scheffler et al. 2016; Jo et al. 2018). The high density, vast range, and presence of the insular populations make *M. petax* a convenient object for studying intraspecific geographic variability.

However, *M. petax* remains a poorly studied bat species, which is largely due to the fact that *M. petax* was until recently considered as part of the widespread polytypic species *Myotis daubentonii* Kuhl, 1819 (Ognev 1928; Kuzaykin 1950; Gromov et al. 1963; Tiunov 1984, 1997; Yoshiyuki 1989; Bogdanowicz 1994; Koopman 1994), and only in the early 2000s the species rank of *M. petax* was confirmed by molecular (Matveev et al. 2005; Kruskop et al. 2012), karyological (Gorobeyko et al. 2020), and morphological data (Kruskop 2004; Matveev et al. 2005). As a consequence, many details of the lifestyle and ecology of *M. daubentonii* have been extrapolated to *M. petax*, leaving our data on the latter species actually deficient. Furthermore, only a small number of *M. petax* individuals have been included in molecular analyses.

Previously, based on mtDNA COI sequences, it was shown that *M. petax* has low nucleotide variability with a prevalence of the central, most abundant haplotype (Gorobeyko et al. 2020), while the intraspecific p distances between specimens amount to 0.28% to 1.16% (Kruskop et al. 2012; Gorobeyko et al. 2020). The differences between mtDNA cyt *b* sequences of *M. petax* from the Russian Far East and Northeast China are amounted to 0.2% (Wang et al. 2010). At the same time, the coefficient of genetic distances (DL) within *M. petax* calculated on the basis of Inter-SINE(MIR)-PCR data according to Link et al. (1995) range from 0.13–0.55, which may indicate genetic heterogeneity (Matveev et al. 2005).

The Far Eastern specimens of *M. petax* have significant differences in the amount and locality of heterochromatic materials in chromosomes that are not common for the genus *Myotis* (Gorobeyko et al. 2020). Another unusual trait of *M. petax* is the presence of short, 30 bp R1 repeats in the control region of mtDNA found in individuals from the Amur Region and Primorsky Territory of Russia (Gorobeyko et al. 2023). Long, 81 bp R1 repeats in *M. petax* are presented in a variable copy number (4–7), exhibit inter-individual sequence diversity, and consist of parts of the ETAS1 and ETAS2 conservative blocks of mtDNA. The size heteroplasmy previously described for *Myotis* species was not detected in *M. petax* (Gorobeyko et al. 2023).

The following subspecies have been described for the species based on morphometric characters: nominotypical, common in Western Siberia; *M. p. ussuriensis* Ognev, 1927 inhabiting the Far East; *M. p. loukashkini* Shamel, 1942, and *M. p. chasanensis* Tiunov, 1997, whose ranges need to be clarified (Tiunov 1997; Kruskop 2004; Tiunov and Makarikova 2007; Wang et al. 2010; Gorobeyko et al. 2021). In addition, an analysis of the morphometric variability of *M. petax* revealed the presence in the Russian Far East of the "Amurian morphological form" which differs from the formerly known subspecies by a combination of craniometric parameters (Gorobeyko et al. 2021). It is important to take into account that only *M. p. loukashkini* was described as a subspecies of *M. petax* (Shamel 1942), whereas the identification of the subspecies *M. p. ussuriensis* and *M. p. chasanensis* was based on the differences of these morphological forms from *M. daubentonii* sensu lato. Therefore, it appears that the validity of subspecies and the intraspecific structure of *M. petax* are still unclear.

Given the above context, the goal of this study was to ascertain the intraspecific structure of *M. petax* by examining their genetic and morphological structures. Accordingly, we analyzed the control region of mtDNA and craniometric variability for an extensive sample from the entire range, which made it possible to define *M. petax* intraspecific structure for the first time. We then discuss the correspondence of *M. petax* subspecies to genetic lineages and their possible contact zones of different forms.

Material and methods

Bat sampling

Bats were captured in July-August in summer roosts, from June to September in foraging sites, and in May and August-September in swarming sites (at cave entrances) using mist nets (6.0/7.0/10.0 m × 2.5 m, Ecotone, Poland) (Fig. 1). In April and between November and December, bats were captured by hand in hibernation sites. The short information about sampling localities in different regions with assigned codes is listed in Table 1 and is detailed in the Supplementary Information (Suppl. material 1: table S1). Bat wing membrane biopsies were sampled by a 3 mm skin biopsy punch, bat wing membrane biopsies were taken and preserved in 96% ethyl alcohol at -20°C until DNA was extracted. The bats were then released at their capture sites the next evening after being ringed with 2.9 mm aluminum rings. The sample material is stored in the Bioresource Collection of the Federal Scientific Centre of East Asia Terrestrial Biodiversity of

the Far East Branch of the Russian Academy of Sciences (reg. number 2797657). Tissue samples (muscle) from bat vouchers (carcasses fixed in ethanol) deposited at the Zoological Museum of Lomonosov Moscow State University (ZMMU, Moscow, Russia), the Institute of Biological Problems of the North (Far Eastern Branch of the Russian Academy of Sciences, Magadan, Russia), and Surgut State University (Surgut, Russia) were also used. All applicable international, national and institutional ethics statements involving animals in research have been followed. Approval was granted by the Commission for the Regulation of Experimental Research (Bioethics Commissions) of Federal Scientific Center of the East Asia Terrestrial Biodiversity (Date 25.04.2022/No. 1).

DNA extraction, amplification, sequencing

Total DNA was isolated from ethanol-fixed tissues by the method of saline extraction (Aljanabi and Martinez 1997) or using the Diatom DNA Prep 200 Kit (Isogene Lab., Moscow, Russia), according to the manufacturer's protocol with modifications as described in Kazakov et al. (2020).

The partial control region of mtDNA (from 985 to 1444 bp length) was amplified as in Gorobeyko et al. (2023), and an additional forward primer MPCR-3 (5'-ATCATTCTAATACCACTAACTA-3') with an annealing temperature of 52°C was also used. PCR products were visualized on 1.0% agarose gels, purified using polyethylene glycol (Schmitz and Riesner 2006) or the Cleanup S-Cap Kit (Evrogen JSC, Russia), and sequenced in both directions using the ABI BigDye Terminator v 3.1 Cycle Sequencing Kit with the same primers on an ABI 3500 Genetic Analyzer at the University of Tyumen (Tyumen, Russia) and on an ABI Prizm 3130 Genetic Analyzer (Applied Biosystems, United States) at the Federal Scientific Center of the East Asia Terrestrial Biodiversity (Far Eastern Branch of the Russian Academy of Sciences, Vladivostok, Russia).

Phylogenetic analysis and genetic variability evaluation

The original sequences are deposited in the GenBank database under accession no. OP168765–OP168790, PP447735–PP447836, PP447858–PP447861, PP447863–PP447866, PP447869, PP447872–PP447905. Geographic coordinates and metadata for each individual are given in Suppl. material 1 (Suppl. material 1: table S1). The sequences were aligned with published *M. petax* sequences from the GenBank: KT199099–KT199102 (Hwang et al. 2016), JF806312 (Lu et al. 2013) using the BioEdit, version 7.0.9.0 software or the CLUSTAL algorithm (Sievers et al. 2011). Since the sequences of the *M. petax* control region vary in length from 985 to 1444 bp mainly due to the different number of long tandem repeats and the application of

Figure 1. The Eastern water bat in its natural habitat. *Myotis petax* from Transbaikal Territory, Chikoy River Valley (**A**) and Soktuy-Milozanskaya Cave (**B**), Primorsky Territory, foothills of the Chernye Gory Range (**C**) and Republic of Buryatia, Dolganskaya Yama Cave (**D**). Photo by D.V. Kazakov.

Table 1. Codes for sample collection localities. Genetic – sampling localities for molecular-genetic analysis, Morphology – sampling localities for craniometric analysis, N – number of samples. R – Russian Federation, C – China, K – Kazakhstan, M – Mongolia, SK – Republic of Korea.

Locality	Coordinates	Genetic		Morphology	
		Code	N	Code	N
R: Khanty-Mansi Autonomous Okrug, Korliki village	61°31.20'N, 82°25.20'E	**1**	3		
R: Novosibirsk Region, Barsukovskaya Cave	54°22.20'N, 83°58.20'E	**2**	1		
R: Novosibirsk Region, Novososedovskaya Cave	54°39.00'N, 83°58.80'E			**NN**	4
K: East K Region, Bukhtarma River	49°44.40'N, 83°59.40'E			**KB**	3
K: East K Region, Markakol Lake	48°45.00'N, 85°45.00'E			**KM**	1
R: Altai Territory, Tigireksky Nature Reserve, M. Tigirek River	51°8.40'N, 83°3.00'E	**3**	6		
R: Altai Republic, Kuyum River, Verchne-Kuyumskaya Cave	51°37.80'N, 86°19.80'E			**AK**	1
R: Altai Republic, Altai Nature Reserve	50°52.20'N, 88°57.00'E			**AA**	4
R: Altai Republic, Altai Nature Reserve, Iogach Village	51°46.80'N, 87°15.00'E			**AI**	1
R: Altai Republic, Altai Nature Reserve, Teletskoye Lake	51°31.80'N, 87°42.60'E			**AT**	2
R: Republic of Khakassia, Abakan River	53°36.60'N, 91°31.20'E			**KS**	1
R: Republic of Tyva, Tore-Hol Lake	50°1.80'N, 95°4.20'E			**TY**	11
R: Irkutsk Region, Tayshet City	55°55.80'N, 97°55.80'E	**4**	3	**IT**	3
M: Uvurkhangai aimag, Orhon River	47°6.00'N, 102°46.20'E	**5**	4	**MO**	5
R: Irkutsk Region, Argaley-3 Cave	53°27.00'N, 103°6.00'E	**6**	3		
R: Irkutsk Region, Kultuk village	51°43.80'N, 103°43.80'E	**7**	3	**IK**	
R: Irkutsk Region, Cheremkhovsky District, Oganai River	53°8.40'N, 103°5.40'E			**IO**	1
R: Irkutsk Region, Listvenichny station, Baikal Lake	51°51.00'N, 104°42.60'E	**8**	3		
R: Irkutsk Region, Okhotnichya Cave	52°7.80'N, 105°27.00'E	**9**	4		
R: Irkutsk Region, Mechta Cave	52°57.00'N, 106°46.80'E	**10**	3		
M: Selenge aimag, Orhon River	50°3.60'N, 106°8.40'E	**11**	1		
R: Republic of Buryatia, Bayan village, Dzhida River	50°31.80'N, 105°15.60'E	**12**	3		
R: Republic of Buryatia, Tasarkhay village, Dzhida River	50°31.80'N, 105°30.00'E	**13**	4		
R: Republic of Buryatia, Babushkin City, Mysovka River	51°42.00'N, 105°52.20'E	**14**	3		
R: Republic of Buryatia, Yagodnoe village	51°24.60'N, 106°28.80'E	**15**	1		
R: Republic of Buryatia, Gusinoe Lake	51°17.40'N, 106°26.40'E	**16**	1		
R: Republic of Buryatia, Mostovka village, Selenga River	52°7.20'N, 107°1.80'E	**17**	3		
R: Republic of Buryatia, Ulady village, Kudara River	50°10.80'N, 107°39.00'E	**18**	4	**BK**	3
R: Transbaikal Territory, Zakharovo village, Shiviya River	50°31.80'N, 109°19.80'E	**19**	1		
R: Transbaikal Territory, Shimbilik village	50°32.40'N, 109°35.40'E	**20**	2		
R: Transbaikal Territory, Steklozavod village, Bobrovka River	50°34.80'N, 110°13.20'E	**21**	3		
R: Transbaikal Territory, 10 km S of Khilogoson village, Arey River	51°3.00'N, 110°37.20'E	**22**	1		
R: Republic of Buryatia, Dolganskaya Yama Cave	54°26.40'N, 113°46.80'E	**23**	11	**BD**	4
R: Transbaikal Territory, Soktuy-Milozanskaya Cave	50°1.80'N, 117°55.20'E	**24**	5		
C: Inner Mongolia, Dalainor Lake	48°58.20'N, 117°25.80'E			**CI**	2
M: Dornod aimag, Khalkhyn-Gol River	47°36.00'N, 118°45.60'E	**25**	6	**MK**	7
R: Transbaikal Territory, Shilka River	53°25.20'N, 120°19.80'E			**TS**	2
R: Sakha Republic (Yakutia), Buotama River	61°15.00'N, 128°45.00'E	**26**	3		
R: Amur Region, Sosnovyi Bor village	53°45.60'N, 126°53.40'E	**27**	9	**ZE**	25
R: Amur Region, Tokinsko-Stanovoy National Park	55°37.80'N, 130°42.00'E	**28**	2		
R: Amur Region, Khingansky Nature Reserve, Dolgoe Lake	49°21.60'N, 129°45.60'E	**29**	10	**AR**	23
R: Amur Region, Khingansky Nature Reserve, Gryaznaya River	48°54.00'N, 130°30.60'E			**AG**	1
C: Heilongjiang, Hailin	44°33.60'N, 129°22.80'E			**CH**	2
R: Khabarovsk Territory, Talandin adits	50°50.40'N, 137°28.80'E	**30**	2	**HT**	2
R: Khabarovsk Territory, Galichnyi village	50°42.00'N, 137°12.00'E	**31**	10	**HG**	5
R: Khabarovsk Territory, Proschalnaya Cave	47°18.60'N, 136°30.00'E	**32**	4	**HP**	3
R: Primorsky Territory, Spasskaya Cave	44°34.80'N, 132°46.20'E	**33**	2	**PS**	2
R: Primorsky Territory, Lazovsky Nature Reserve, Korpad cordon	43°15.60'N, 134°1.80'E	**34**	5		
R: Primorsky Territory, Primorsky Velican Cave	43°16.20'N, 133°37.20'E	**35**	7	**PV**	8
R: Primorsky Territory, Ussuriysk City	43°48.00'N, 131°57.00'E			**PU**	2
R: Primorsky Territory, LZP-3, Priiskovaya Cave	44°22.80'N, 133°12.00'E			**PP**	6
R: Primorsky Territory, Barabashevka River	43°14.40'N, 131°21.60'E	**36**	1	**PB**	1
R: Primorsky Territory, Ryazanovka River	42°49.20'N, 131°14.40'E	**37**	2	**PR**	2

Locality	Coordinates	Genetic		Morphology	
		Code	N	Code	N
R: Primorsky Territory, Tsukanovka River	42°46.80'N, 130°48.00'E	**38**	10	**PT**	10
R: Primorsky Territory, Mayachnoe village	42°38.40'N, 130°41.40'E	**39**	4	**PM**	4
R: Primorsky Territory, Kraskino village	42°42.60'N, 130°46.80'E			**PK**	1
R: Primorsky Territory, Khasan Lake	42°27.00'N, 130°36.60'E			**HA**	17
R: Primorsky Territory, Golubiny utyos	42°24.60'N, 130°45.00'E	**40**	4		
R: Sakhalin Island, Pilenga River	50°58.20'N, 142°52.80'E	**41**	1		
R: Sakhalin Island, Lesnaya River	48°34.80'N, 142°43.80'E	**42**	2		
R: Sakhalin Island, Listvennitsa River	47°34.80'N, 142°36.00'E	**43**	1		
R: Sakhalin Island, Pukhovaya River	47°28.80'N, 142°37.20'E	**44**	2		
R: Sakhalin Island, Kitosiya River	46°22.20'N, 141°52.20'E			**SK**	4
R: Sakhalin Island, Plelyarna River	51°19.80'N, 143°13.20'E			**SN**	1
R: Sakhalin Island, Poronaiysky District	49°52.20'N, 143°58.20'E			**SP**	1
R: Iturup Island	44°60.00'N, 147°52.80'E			**IP**	2
R: Kunashir Island, Andreevka River	43°53.40'N, 145°37.20'E	**45**	1	**KA**	2
R: Kunashir Island, Ozernaya River	43°52.20'N, 145°28.80'E	**46**	2	**KO**	2
R: Kunashir Island, Severyanka River	44°20.40'N, 146°0.60'E	**47**	3		
C: Jilin Province, Ji'an City	41°7.50'N, 126°11.64'E	**48**	1		
SK: Gangwon Province	37°19.80'N, 128°9.60'E	**49**	4		

different primer pairs, we used only an 833 bp length part of the control region sequences for phylogenetic reconstruction and to construct a haplotype network. Additional R1 repeats and a portion of the middle repeats in individuals with more than 2 middle repeats were excluded to achieve equal sequence length. *Myotis fimbriatus* and *M. pilosus* sequences (JF806303, Lu et al. 2013; MN245054, Hao 2019) from the GenBank database were used as outgroups.

Maximum likelihood reconstruction was conducted in the IQTREE v. 1.6.12 software (Nguyen et al. 2015) with 1000 bootstrap replicates to test topology stability. ModelFinder (Kalyaanamoorthy et al. 2017) was used to select the optimal partitioning scheme and the best-fit substitution model under the BIC criterion: TN+F+I+G4 (Tamura and Nei 1993). The Bayesian tree was constructed in BEAST 2.0 software by Bayesian inferences performed for 10×10^6 generations (Bouckaert et al. 2019). Branches with bootstrap supports and posterior probabilities greater than 70% were considered reliable. Median-joining haplotype network was constructed using NETWORK v. 10.2 (https://www.fluxus-engineering.com/). Metrics of genetic diversity were calculated using DnaSP 6.12 (Rozas et al. 2017) and ARLEQUIN v. 3.5 (Excoffier and Lischer 2010).

Morphological analysis

A preliminary morphometric analysis was performed by us earlier (Kruskop 2004; Gorobeyko et al. 2021); here we expanded the sample with individuals from previously unrepresented regions throughout the range of *M. petax*. A total of 168 *M. petax* specimens (skulls, extracted from dry or alcohol-preserved skins) were measured and further analyzed. The complete list of the specimens examined with their corresponding localities and coordinates, is provided in the Supplementary Information (Suppl. material 1: tables S1, S2).

The following 15 craniodental measurements were taken: **CBL** – condylobasal length, **CCL** – condylocanine length, **MW** – mastoid width of skull at the level of the auditory bullae, **BCW** – width of braincase, **BCH** – height of braincase, **IOW** – interorbital width, **RL** – rostral length from anteorbital foramen to the alveolus of the inner incisor, **RW** – rostral width at the level of the infraorbital foramina, **C1C1** – crown-measured width between the outer margins of upper canines, **M3M3** – crown-measured width between outer margins of **M3**, **C1M3** – **C-M3** length, **IM3** – maxillary row length, **C** – length of the upper canine cingulum base, **M3L** – crown length of **M3**, **M3W** – crown width of **M3**, **MdL** – length of the lower jaw to the posterior edge of the angular process. The scheme for performing skull measurements is given in Suppl. material 2. The measurements were taken under a binocular using an electronic caliper with an accuracy of 0.01 mm. Morphometric analyses were performed using the appropriate modules of STATISTICA for Windows version 7.0 (StatSoft, Inc., 2004). All data were standardized before analysis.

Morphometric analysis was carried out in several stages. At the first stage, an analysis of sexual dimorphism was conducted, for which total samples of males (n=62) and females (n=79) were compiled, and the average values of the parameters were analyzed. It was noted that the distribution of all the parameters under study was normal; hence, the Student's t-test was used to determine whether sexual dimorphism was present for each parameter (differences were considered significant at $p < 0.01$).

Next, to analyze geographic variation, cluster analysis was conducted for the entire undivided sample, as well as stepwise discriminant function analysis (DFA) for local samples. For each local sample, the mean measurement values (M), minimum and maximum values (min and max), as well as the standard error of the mean (SE), variance (σ), and coefficient of variation (CV) were calculated. Kruskal-Wallis analysis of variance (ANOVA) was

performed to assess similarities and differences for local samples because the distribution was different from normal. A comparison of average ranks (z) and p' revealed local samples that did not differ from each other in any characteristic (differences were considered significant at p'<0.01), and after several rounds of ANOVA, they were combined into a larger learning samples for further DFA.

The DFA was performed in four rounds using the learning samples and a sample named UN (undefined), which included specimens not examined in previous analyses. Stepwise DFA using learning samples is described in detail in previous works (Matveev et al. 2005; Gorobeyko et al. 2021). The squared Mahalanobis distances between the learning samples and the level of p-significance, as well as posterior probabilities for each specimen, were calculated. A comparison of classification matrices with the results of canonical analysis made it possible to match individuals from the UN with one or another learning sample and combine them into larger groups. The mean measurement values (M), minimum and maximum values (min and max), as well as the standard error of the mean (SE), variance (σ), and coefficient of variation (CV), were calculated for groups obtained after five rounds of DFA.

Results

Tandem repeats and sequence length variability

In this work, partial sequences of the mtDNA control region are obtained for 171 *M. petax* specimens from 48 localities. The length of the obtained sequences varies from 985 to 1444 bp, mainly due to the copy number of the repeats varying from 4 to 8 among individuals. One or two short 30 bp additional R1 repeats in the control region of mtDNA are found in the individuals from the Amur Region, Primorsky Territory, Transbaikal Territory, and Irkutsk Region.

Small insertions of 1–15 bp length, duplicating the part of the ETAS-domain, were detected at the beginning of the control region in one specimen from the Khabarovsk Territory and four individuals from the Republic of Buryatia and in the last R1 repeats in two individuals from the Altai Territory.

Additional data on sequence length variability are detailed in the supporting information (Suppl. material 3).

Phylogenetic analysis and distribution of genetic lineages

Five highly differentiated genetic lineages are identified both on the ML tree and the Bayesian tree (Fig. 2). All lineages are well separated and highly supported, but the topology of both phylogenetic trees differs in detail. The median-joining haplotype network also showed the presence of five genetic lineages that are in good agreement with those identified on the phylogenetic trees (Fig. 3).

The two most genetically divergent lineages are "Korea" (n=4) and "Kunashir" (n=6), named after the only localities where these lineages were found, i.e., the Korean Peninsula and Kunashir Island, respectively. Although the position of these clades on the ML tree is unresolved, on the Bayesian tree lineage "Korea" appears to be more separated from other lineages including lineage "Kunashir."

The relative positions of the lineages "Okhotsk," "Amur," and "Siberia" on the Bayesian tree and the ML tree are different. Moreover, on the Bayesian tree, the lineage "Amur" is closer to the lineage "Siberia" than to the "Okhotsk," while on the ML tree, the lineages "Okhotsk" and "Amur" are more related to each other than to the lineage "Siberia" (Fig. 2). The phylogenetic tree position of one individual OP168767 from Spasskaya Cave (Primorsky Territory) is unclear, since on the ML tree and MJ network it is more related to the lineage "Okhotsk," although on the Bayesian tree it appears closer to the lineage "Amur".

The approximate range of the lineage "Siberia" (n=103) consists of the western and eastern parts; the first one extends from the upper and middle reaches of the Ob River and the northwestern Altai Mountains west to the Yablonovy Range, south to central Mongolia (Orhon River). The eastern part comprises the southern Sikhote-Alin Mountains and foothills of the Chernye Gory Range (Primorsky Territory). The single individuals of this lineage are also found in the Khabarovsk Territory: central Sikhote-Alin Mountains (1 out of 4 specimens) and Lower Amur (1 out of 12 specimens). Specimens from the Selenga Valley (Republic of Buryatia, Transbaikalia Territory), the Chernye Gory Range, and the Sikhote-Alin Mountains (Primorsky Territory) form three separate clades within the lineage "Siberia," also well supported on the phylogenetic trees.

The lineage "Okhotsk" (n=28) is distributed from central Sikhote-Alin and Lower Amur (Khabarovsk Territory) to the middle reaches of the Lena River (Republic of Yakutia) in the northwest, as well as Sakhalin Island. The single specimens were recorded in the south of the Sikhote-Alin Mountains, in the lower reaches of the Tumannaya River (Primorsky Territory), and in the Jilin Province of China (JF806312). The individuals from the Jilin Province and the Tumannaya River are merged into a single clade based on the Bayesian phylogenetic tree and ML tree.

The estimated range of lineage "Amur" extends from the Yablonovy Range and eastern Mongolia (Khalkhyn-Gol River) to the Ussuri River Valley and Lake Khanka in the east, as well as to the Stanovoy Range in the north. A single individual was detected near the Tayshet City of Irkutsk Region (1 out of 4 specimens). Genetic lineage "Amur" is characterized by the presence of 1–2 short additional repeats in the control region. One additional repeat occurs in the samples from the Amur Region (Stanovoy Range, Middle Amur), Irkutsk Region, Primorsky Territory, Transbaikal Territory, and Mongolia. Two additional repeats are found in specimens from the Amur Region (Sosnovyi Bor village) and Transbaikal Territory (Soktuy-Milozanskaya Cave).

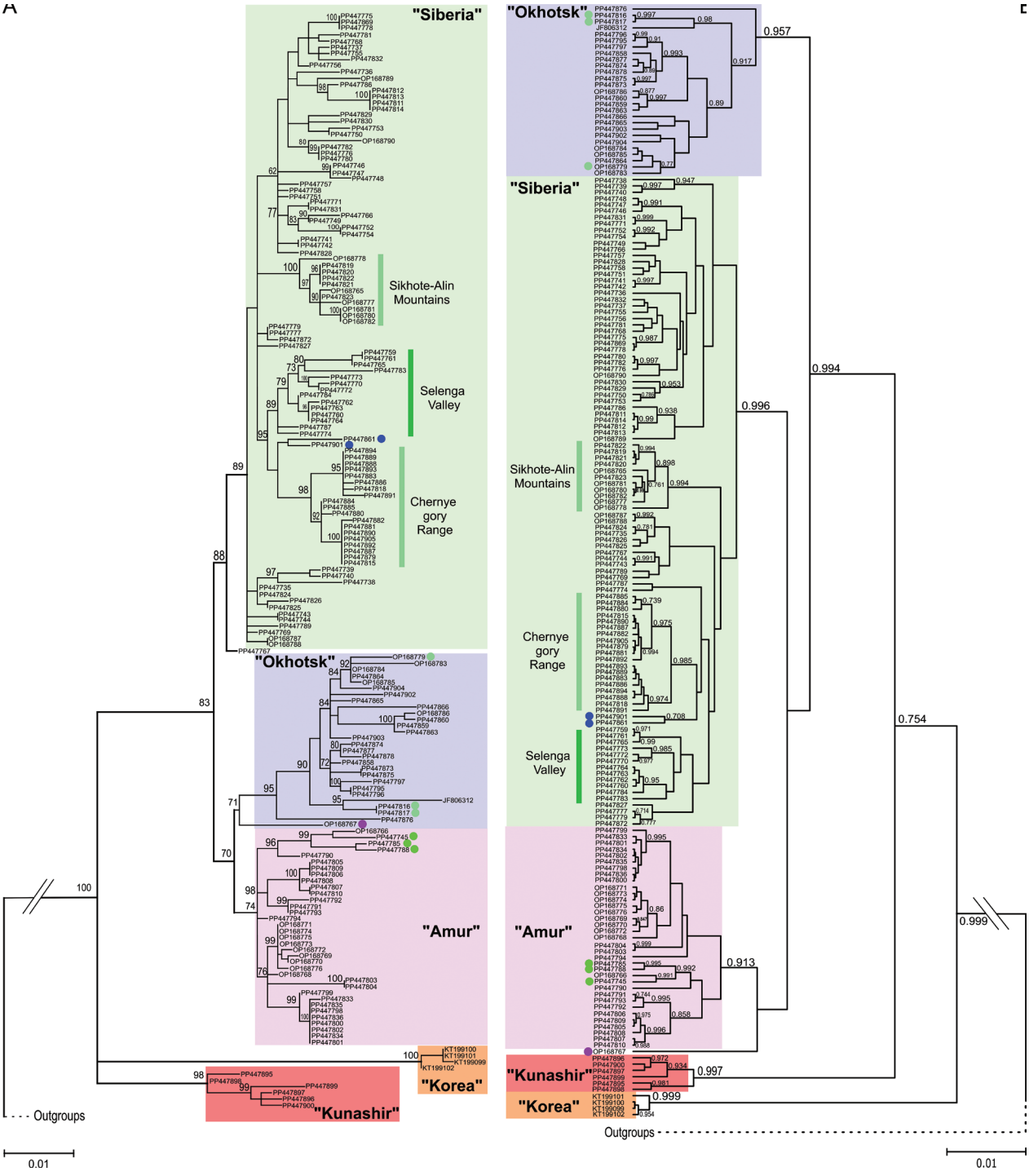

Figure 2. Maximum likelihood (**A**) and Bayesian phylogenetic trees (**B**) based on control region sequences of *Myotis petax* and outgroups. Nodes are labeled with the bootstrap support and posterior probabilities values. Circles indicate samples whose locations does not correspond to the approximate ranges of the mitochondrial lineages to which they belong. The circle color corresponds to the sampling sites: green – "Siberia," blue – "Okhotsk," purple – "Amur." The ID accession nos. for the sequences used in the phylogenetic analysis are listed in the Suppl. material 1: table S1. The substitution model used in the Maximum Likelihood Tree was TN+F+I+G4 with 1000 bootstrap replicates, and the Bayesian tree was constructed using the Bayesian inferences performed for 10×10^6 generations.

Intraspecific genetic diversity

Mean p distances within genetic lineages vary from 0.80% to 1.12%, and K2P distances are 0.88–1.15%. Mean p distances between different lineages varied from 1.84% to 4.76%, and K2P distances were from 1.88% to 5.00%. A comprehensive table that details the within- and between-group distances can be found in the Supplementary Information (Suppl. material 1: table S3).

Genetic diversity indicators for different genetic lineages, geographical regions, and the entire sample are shown in Table 2. The lowest nucleotide diversity and average number of pairwise nucleotide differences (0.017 and 1.5) were found in the lineage "Korea" and the highest in the lineages "Siberia" (0.0111 and 9.836)

and "Okhotsk" (0.0117 and 10.302). The level of nucleotide diversity and average number of pairwise nucleotide differences within the entire sample are higher than in separate genetic lineages (0.0186 and 16.339), which indicates a large contribution of intergroup differences to intraspecific variability. Haplotype diversity values are high and range from 0.833 to 1. The values of Tajima's test are negative, but only for the lineages "Okhotsk" and "Siberia" are statistically significant ($p<0.01$). The values of the Fu test coefficient are not statistically significant.

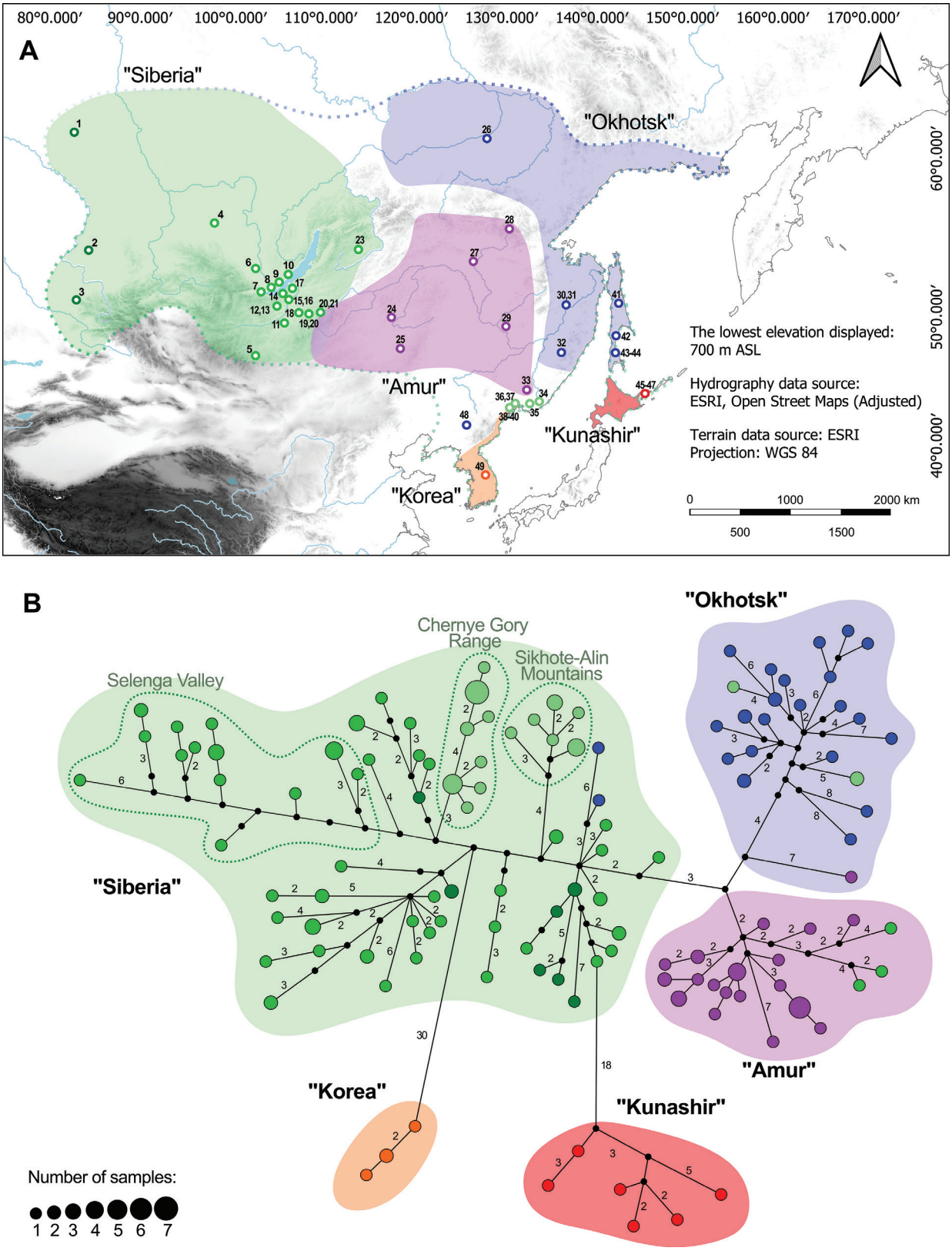

Figure 3. Approximate ranges of genetic lineages (green, purple, blue, orange and red shaded areas) and sampling sites. For site numbers, see Table 1 and Supplementary Information (**A**). Median-joining network of control region haplotypes in *Myotis petax* (**B**); color-coded based on their geographical areas and numbers represent connections separated by more than one mutation.

Indicator of demographic expansion is relatively higher in the lineages "Siberia" and "Okhotsk," but lower than in the entire sample, while spatial expansion in the lineages "Siberia," "Kunashir" and "Okhotsk" is higher compared to the entire sample. Lineage "Korea" is characterized by the lowest values of demographic expansion and spatial expansion indicators.

Morphological variability

In the first phase, we compared the average values of craniometric parameters in the total samples of males (n=62) and females (n=79) to ensure the absence of sexual dimorphism. No significant differences (p>0.01) were found between females and males for any of the studied measurements, which allows the use of samples not separated by sex in further analysis of geographical variability.

For this purpose, 168 individuals from 41 localities are combined geographically into 18 local samples: **INS** – Kuril Islands (**IP**, **KA**, **KO**); **SAH** – Sakhalin Island (**SK**, **SP**, **SN**); **KHASAN** – Lake Khasan (**HA**), **KHAS** – Khasan District of Primorsky Territory (**PB**, **PR**, **PT**, **PK**, **PM**), **PRI** – the rest part of Primorsky Territory (**PB**, **PS**, **PU**, **PP**); **KHAB** – south of Khabarovsk Territory (**HP**), **KOM** – middle part of Khabarovsk Territory (**HT**, **HG**); **AMU** – south of Amur Region (**AR**, **AG**), **ZEA** – north of Amur Region (**ZE**); **CHI** – China (**CI**, **CH**); **ZAB** – Transbaikalia Territory (**TS**); **BUR** – Republic of Buryatia (**BK**, **BD**), **IRK** – Irkutsk Region (**IT**, **IO**, **IK**), **MON** – Mongolia (**MO**, **MK**), **TYV** – Republic of Tyva (**TY**), **ALT** – Republic of Altai (**AA**, **AT**, **AI**, **AK**), **KAZ** – Kazakhstan (**KB**, **KM**), **SIB** – Novosibirsk Region and Republic of Khakassia (**NN**, **KS**). Codes of localities are given in Table 1. The division of individuals from Primorsky and Khabarovsk Territories and the Amur Region into several local samples is dictated by the results of a preliminary morphometric analysis (Gorobeyko et al. 2021), which showed that these regions may be a contact zone for several morphological subspecies. The process of sequentially combining local samples using Kruskal-Wallis ANOVA and learning samples in a stepwise analysis of discriminant functions is reflected in Figure 4 and Suppl. material 1 (Suppl. material 1: table S2).

Figure 4. Sequential integration of local samples in the DFA of geographic variability after Kruskal Wallace analysis. Abbreviations for local and learning samples are given in the text.

In the first run, a DFA was performed with the next learning samples: KHASAN, ZEA, KOM, WSIB (Western Siberia, including ALT, KAZ, SIB, TYV), FE (Far East, including KHAB, INS, PRI, SAH), and BAI (Baikal, including BUR, IRK, ZAB). The following samples are included as UN (undefined): CHI, KHAS, MON, and AMU. In the next two rounds of DFA, no significant differences were found between BAI and ZEA, which allowed combining these samples into UAMU (Upper Amur); on the contrary, several individuals of AMU were assigned to KOM. During the IV round of DFA, it was found that specimens of KHAB are more likely to be assigned to the AMUR group than to the FE group, resulting in the KHAB being classified as the Baikal-Amur group in the final round of DFA.

As a result of the canonical analysis of the final samples, five morphological groups were obtained: "Far East," "Khasan," "Baikal-Amur," "Western Siberia," and "Lower Amur" (inner circle in Fig. 4) and designated by the names of the geographic regions where these forms were discovered. On a scatter diagram, the morphological groups are divided by the first canonical variate into two separate clusters without overlapping (Fig. 5A). The Khasan and Lower Amur groups are part of the first cluster, while the Far East, Baikal-Amur, and Western Siberia groups are part of the second. The groups of the first cluster are well separated by the third canonical variate (Fig. 5A), while the second cluster groups are highly overlapped (Fig. 5B). A map of the expected distribution of morphological forms is presented in Figure 5C.

The Mahalanobis distances and p values for each morphological group (A) or values for groups of the second cluster (B) are displayed in Table 3A–B. Classification matrices displaying the percentage of individuals correctly identified in the DFA and the number of individuals that could be classified into another group are given in Table 3C and Table 3D (for the second cluster groups only). For each morphological group, the percentage of correct identification of individuals is quite high, which is also confirmed by reliable p-level values between groups. The average Mahalanobis distances between groups within both clusters were relatively small (4.73–8.79), but between groups in different clusters, the distances were an order of magnitude higher (41.37–53.11).

Standardized canonical discriminant function coefficients of each are given in Suppl. material 1 (Suppl. material 1: table S4). The first root has a highly positive correlation with condylobasal length, maxillary row length, mandibular length, and intercanine width and has a negative correlation with condylocanine length, braincase width, and rostrum width. On the contrary, the second root has a positive correlation with condylocanine length, mastoid width, and mandibular length and has a negative correlation with braincase width, rostral length, and canine base width. The third root has a positive correlation with condylocanine length, interorbital width, intermolar width, and maxillary row length and has a negative correlation with mastoid width, braincase width, and rostrum width.

Canonical analysis, conducted only for groups of the second cluster, showed a significantly better division of the Far East, Baikal-Amur, and Western Siberia groups according to the first and second roots (Figure 5B). Standardized canonical discriminant function coefficients of each root are given in Suppl. material 1 (Suppl. material 1: table S4).

The mean, minimum, and maximum measurement values; standard error of the mean; variance; and coefficient of variation for each of the morphological groups and the entire sample are presented in Table 4. Almost all of the measurements overlap between different morpholog-

Table 2. Indicators of genetic diversity for genetic lineages and different geographic regions. n – sample size; N – number of haplotypes; Vs – number of variable sites; k±SE – average number of pairwise nucleotide differences; h±SD – haplotype diversity; π±SD – nucleotide diversity; Tajima's D – coefficient of Tajima's test (statistically significant values ($p<0.01$) are highlighted in bold); Fu's Fs – Fu test coefficient; τd and τs are indicators of demographic expansion and spatial expansion, respectively (expansion time in mutation units); SE – standard error, SD – standard deviation. * The sample "Siberian" includes specimens from the localities Nos 1–18, 23. Geographical regions whose nucleotide diversity value is significantly higher compared to neighboring territories are highlighted in bold.

Genetic lineages						
	"Amur"	**"Okhotsk"**	**"Siberia"**	**"Kunashir"**	**"Korea"**	**Total**
n	35	28	103	6	4	176
N	21	24	69	6	3	123
Vs	44	69	107	18	3	183
k±SE	7.644±0.765	10.302±1.688	9.836±0.401	7.067±4.829	1.500±0.536	16.339±0.609
h±SD	0.945±0.024	0.989±0.012	0.988±0.004	1±0.096	0.833±0.222	0.993±0.0017
π±SD	0.0087±0.0008	0.0117±0.0012	0.0111±0.0004	0.0080±0.0014	0.0017±0.0006	0.0186±0.0008
Tajima's D	-1.087	**-1.666**	**-1.715**	-0.644	-0.754	-1.589
Fu's Fs	-5.385	-10.578	-54.391	-1.521	-0.288	-106.084
τ_d	4.713	6.888	8.585	6.141	1.5	9.509
τ_s	6.127	6.416	9.672	7.983	1.299	6.300
Geographical regions						
	Sakhalin Island	**Primorsky Territory**	**Khabarovsk Territory**	**Amur Region**	**Transbaikal Territory**	**Siberian***
n	6	35	16	20	12	60
π±SD	0.0080±0.0027	**0.0134±0.0014**	**0.0118±0.0016**	0.0050±0.0007	**0.0134±0.0013**	0.0097±0.0005

ical groups. The most variable measurements are dental characteristics such as canine base width and length of the 3rd molar base, with the coefficient of variation from 7.445 to 10.866. The width of the 3rd molar base is slightly less variable with a coefficient of variation from 4.766 to 6.994. The rostral length may be slightly variable with a coefficient of variation of 2.878 or moderately variable with a coefficient of variation from 4.092 to 7.117.

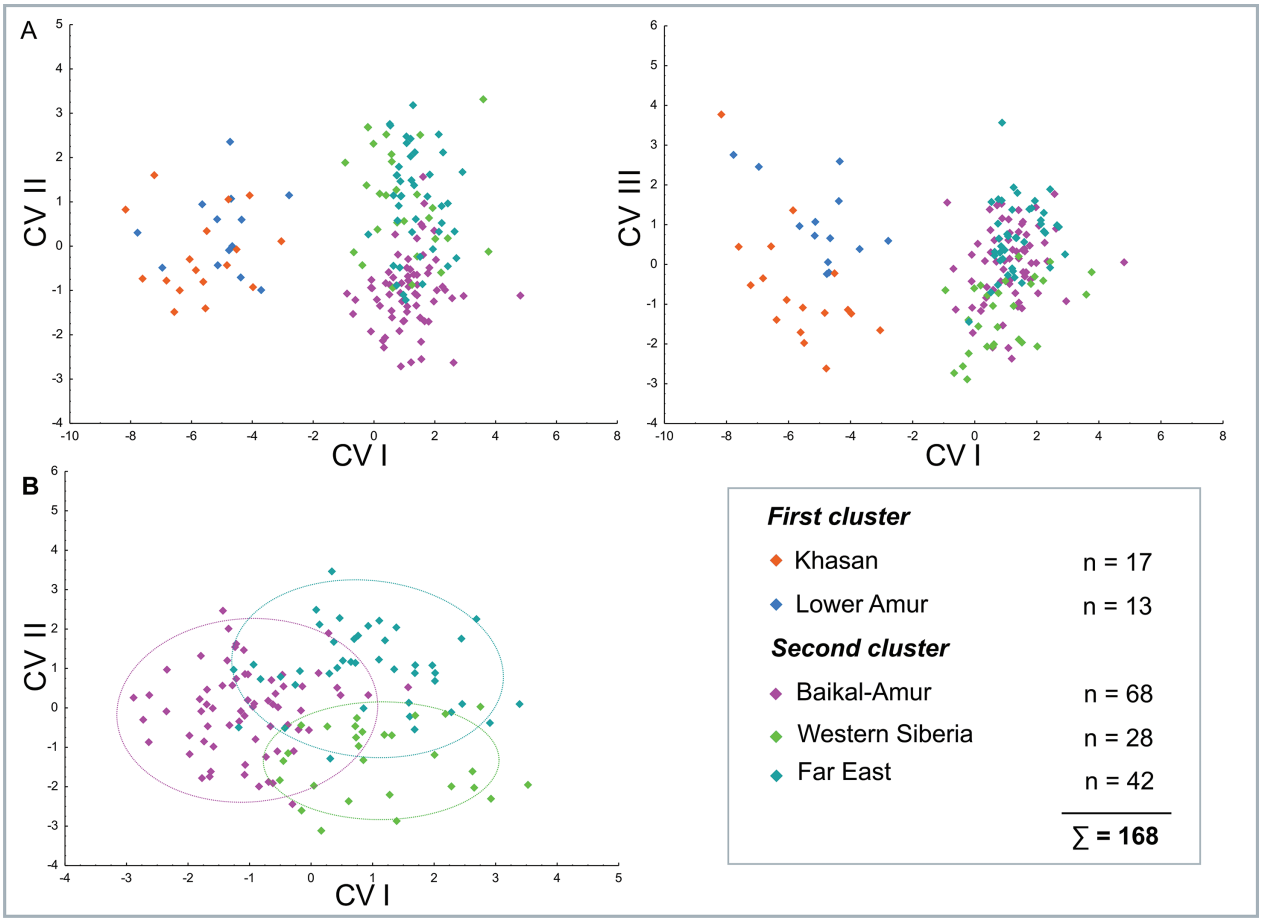

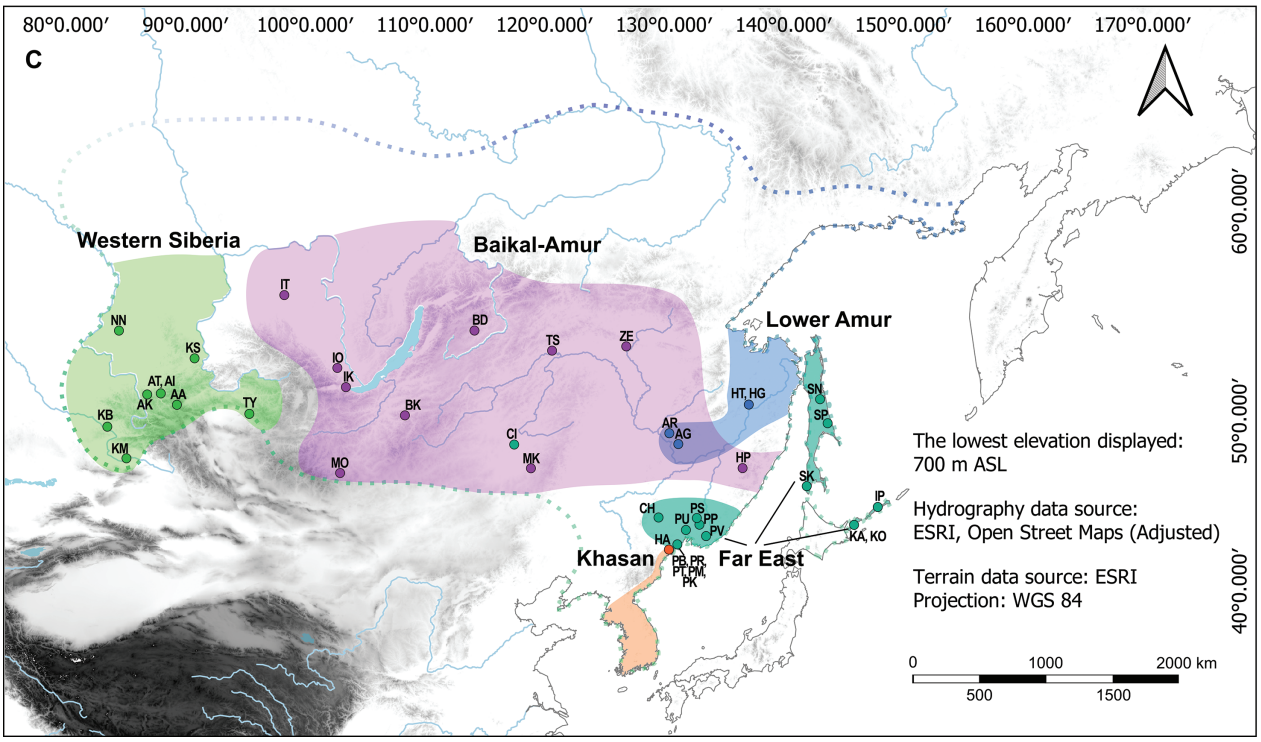

Figure 5. Canonical analysis of the final samples and expected distribution ranges of morphological groups. **A** – all groups are plotted with CV I against CV II and CV III; **B** – only groups of second clusters are plotted with CV I against CV II; **C** – map of expected distribution of morphological form. The colors on map correspond to those on the graphs.

Table 3. Mahalanobis distances, p values and matrix of classification for each morphological group. BAM – Baikal-Amur, SIB – Western Siberia, LAM – Lower Amur, FE – Far East, HAS – Khasan.

A		Mahalanobis distances squared					B		Mahalanobis distances squared		
Groups		BAM	SIB	FE	LAM	HAS	Groups		BAM	SIB	FE
BAM			5.92	42.06	4.86	48.73	BAM			6.37	4.94
SIB		0		4.73	41.37	47.63					
FE		0	0		43.94	53.11	SIB		0		5.5
LAM		0	0	0		8.79					
HAS		0	0	0	0		FE		0	0	0
		p level							p level		
C	Matrix of classification						D	Matrix of classification			
Groups	%	BAM	SIB	FE	LAM	HAS	Groups	%	BAM	SIB	FE
BAM	89.71	61	1	6	0	0	BAM	89.71	61	1	6
SIB	71.43	5	20	3	0	0					
FE	92.31	8	3	31	0	0	SIB	67.86	5	19	4
LAM	73.81	0	0	0	12	1					
HAS	88.24	0	0	0	2	15	FE	73.81	8	3	31
Total	**82.74**	**74**	**24**	**14**	**40**	**16**	**Total**	**80.43**	**74**	**41**	**23**

Table 4. Craniodental measurements for morphological groups of *M. petax*. For abbreviations, see Material and methods.

N	Baikal–Amur				Far East				Western Siberia			
	68				42				28			
	Mean ± SE	min-max	CV	σ	Mean ± SE	min-max	CV	σ	Mean ± SE	min-max	CV	σ
CBL	13.46±0.03	12.89–14.02	1.733	0.054	13.43±0.04	12.97–14.18	1.858	0.062	13.56±0.05	12.85–13.94	2.053	0.078
CCL	12.56±0.03	11.86–13.07	1.887	0.056	12.58±0.04	12.15–13.29	1.945	0.060	12.66±0.05	11.90–13.11	2.290	0.084
MW	7.59±0.01	7.34–7.90	1.598	0.015	7.58±0.02	7.29–7.88	2.120	0.026	7.79±0.03	7.43–8.11	2.001	0.024
BCW	7.43±0.02	7.08–7.82	2.065	0.024	7.32±0.03	7.06–7.73	2.539	0.035	7.53±0.04	7.15–7.88	2.682	0.041
BCH	5.19±0.02	4.88–5.60	3.005	0.024	5.32±0.04	5.00–6.37	4.629	0.061	5.34±0.04	4.84–6.15	4.443	0.056
IOW	3.85±0.02	3.35–4.15	3.544	0.019	3.90±0.02	3.58–4.16	3.083	0.014	3.91±0.03	3.50–4.17	4.087	0.026
RL	6.17±0.03	5.42–6.69	4.092	0.064	5.66±0.06	5.11–6.63	7.117	0.162	5.81±0.08	5.15–6.45	7.075	0.169
RW	4.84±0.02	4.48–5.28	3.126	0.023	4.82±0.02	4.52–5.08	2.575	0.015	4.99±0.03	4.60–5.18	2.874	0.021
C1C1	3.81±0.02	3.19–4.04	3.752	0.020	3.87±0.02	3.66–4.10	2.600	0.010	3.92±0.02	3.66–4.16	2.531	0.010
M3M3	5.58±0.02	5.20–6.09	2.921	0.027	5.65±0.02	5.37–5.87	2.140	0.015	5.63±0.03	5.27–5.92	2.761	0.024
C1M3	5.09±0.01	4.90–5.30	1.826	0.009	5.13±0.02	4.85–5.35	2.215	0.013	5.13±0.03	4.84–5.71	3.407	0.031
IM3	6.15±0.02	5.73–6.36	2.128	0.017	6.16±0.02	5.91–6.54	2.252	0.019	6.20±0.02	5.90–6.54	2.052	0.016
C	0.72±0.01	0.58–0.95	9.549	0.005	0.71±0.01	0.50–0.80	10.260	0.005	0.74±0.01	0.62–0.86	8.750	0.004
M3L	0.80±0.01	0.68–0.99	8.677	0.005	0.77±0.01	0.69–0.98	8.485	0.004	0.78±0.02	0.67–0.92	10.333	0.006
M3W	0.94±0.01	0.81–1.09	6.361	0.004	0.96±0.01	0.85–1.12	5.968	0.003	0.95±0.01	0.86–1.05	4.776	0.002
MdL	10.22±0.04	9.31–10.79	3.144	0.103	10.05±0.05	9.54–11.05	3.525	0.126	10.10±0.07	9.13–10.69	3.799	0.147
N	Khasan				Lower Amur				All			
	17				13				168			
	Mean ± SE	min-max	CV	σ	Mean ± SE	min-max	CV	σ	Mean ± SE	min-max	CV	σ
CBL	13.83±0.08	12.83–14.36	2.470	0.117	14.03±0.09	13.68–14.77	2.245	0.101	13.56±0.03	12.83–14.77	2.441	0.110
CCL	13.27±0.08	12.58–13.76	2.559	0.115	13.51±0.07	12.81–13.85	1.970	0.071	12.73±0.03	11.86–13.85	3.163	0.162
MW	7.57±0.05	7.27–7.94	2.478	0.027	7.67±0.04	7.45–7.98	1.989	0.023	7.63±0.01	7.27–8.111	2.157	0.027
BCW	7.49±0.04	7.13–7.70	1.994	0.022	7.49±0.05	7.14–7.82	2.219	0.028	7.43±0.01	7.06–7.78	2.471	0.034
BCH	5.21±0.05	4.84–5.56	3.735	0.038	5.33±0.03	5.15–5.58	1.987	0.011	5.26±0.02	4.84–6.37	3.939	0.043
IOW	3.93±0.04	3.58–4.23	3.766	0.022	3.94±0.04	3.76–4.22	3.402	0.018	3.89±0.01	3.35–4.23	3.613	0.020
RL	6.01±0.07	5.44–6.51	4.699	0.080	6.05±0.05	5.75–6.29	2.878	0.030	5.96±0.03	5.11–6.69	6.448	0.148
RW	4.93±0.05	4.47–5.53	4.567	0.051	4.86±0.05	4.57–5.13	3.877	0.036	4.87±0.01	4.47–5.53	3.404	0.027
C1C1	3.70±0.04	3.43–4.00	4.209	0.024	3.92±0.08	3.60–4.76	7.257	0.081	3.84±0.01	3.19–4.76	4.117	0.025
M3M3	5.47±0.04	5.19–5.77	2.968	0.026	5.69±0.07	5.39–6.34	4.622	0.069	5.60±0.01	5.19–6.34	3.037	0.029
C1M3	4.78±0.04	4.48–5.14	3.851	0.034	4.89±0.09	3.96–5.16	6.737	0.109	5.06±0.01	3.96–5.71	3.728	0.036
IM3	5.98±0.05	5.60–6.33	3.167	0.036	6.01±0.07	5.36–6.38	4.027	0.059	6.13±0.01	5.36–6.54	2.659	0.027
C	0.74±0.02	0.62–0.93	10.504	0.006	0.76±0.02	0.59–0.90	10.866	0.007	0.73±0.01	0.50–0.95	9.898	0.005
M3L	0.83±0.02	0.70–0.93	8.633	0.005	0.84±0.02	0.72–0.95	7.445	0.004	0.79±0.01	0.67–0.99	9.080	0.005
M3W	1.05±0.02	0.90–1.19	6.773	0.005	1.01±0.02	0.89–1.08	6.243	0.004	0.96±0.01	0.82–1.19	6.994	0.005
MdL	9.67±0.05	9.17–9.97	2.163	0.044	9.74±0.08	9.33–10.28	2.777	0.073	10.07±0.03	9.13–11.05	3.710	0.139

Discussion

It was shown that natural habitats of *M. petax* and, in particular, the foraging sites are closely associated with different types of water bodies (lakes, ponds) and river systems (Tiunov 1997; Botvinkin 2002; Didorenko et al. 2022). The approximate borders of the mitochondrial genetic lineages' distributions appear to coincide with the major watersheds of northeast Asia. So, the eastern border of the mitochondrial lineage "Siberia" and the western border of the lineage "Amur" are apparently the Yablonovy Range and the Khentei-Daurian Highlands, representing watersheds of the Arctic and Pacific oceans (Geniatulin 2009). The northern limit of the mitochondrial lineage "Amur" distribution is the Stanovoy Range, another watershed between the Arctic and Pacific oceans. Thus, the approximate range of the lineage "Amur" generally coincides with the Amur River basin, with the exception of the Lower Amur.

The mitochondrial lineage "Siberia" predominates in the Southern Sikhote-Alin and in the foothills of the Chernye Gory Range (and possibly in the Jilin province of China), while haplotypes of the lineage "Okhotsk" are found here in a mosaic manner. This suggests that the pattern of distribution of these two lineages probably represents a gradient, where in the southern part the haplotypes of the lineage "Siberia" predominate, but further north the ratio changes in the opposite direction, and starting from the central Sikhote-Alin, the haplotypes of the lineage "Okhotsk" are prevalent. Indicators of demographic and spatial expansion in the lineages "Siberia" and "Okhotsk" are higher compared to all other lineages. Combined with statistically significant negative Tajima's D values, this may indicate past population growth with range expansion of these lineages, which, consequently, could lead to the expanding of the contact zone between lineages in Southern and Central Sikhote-Alin.

Due to the lack of genetic data from northeast China, the mitochondrial lineage "Siberia" is assumed to have a significant distribution gap (about 1800 km around). As a result, it is not possible to say unequivocally that the connection between the eastern and western portions of the range is completely interrupted. However, it appears that both parts of the range of the lineage "Siberia" were connected in the past, as has been shown for some Asian species with a ring range (Matyushkin 1976, 1982). Recent findings of *M. petax* in Jiangxi and Guangdong provinces, confirmed genetically (Wu et al. 2022), indicate that the species' range in China may be much wider than previously thought.

The value of nucleotide diversity in the Primorsky Territory, Khabarovsk Territory, and Transbaikal Territory is significantly higher compared to neighboring territories (Table 2), which can be explained by the cohabitation of various genetic lineages at the confluence of different river basins. Thus, in Primorsky Territory, where the rivers of the Amur basin contact with the rivers of the basin of the Sea of Japan (East Sea), we discovered three genetic lineages: "Siberia," "Okhotsk," and "Amur." Two genetic lineages, "Siberia" and "Okhotsk," are found in Khabarovsk Territory, where Amur basin's rivers connect with the rivers of the Sea of Okhotsk basin. The coexistence of "Siberia" and "Amur" lineages occurs in the Transbaikal Territory and Mongolia, where the rivers of the Amur basin relate with the rivers of the Selenga basin. A possible explanation for the presence of individuals of the lineage "Amur" in the Tayshet City could be incomplete sorting of mitochondrial lineages, but this issue requires further research. Although there are no reliable data on the migratory activity of *M. petax*, the ecologically similar Western Palearctic species *M. daubentonii* is considered a sedentary species or a local migrant, but is capable of covering distances of 280–300 km (Hutterer et al. 2005), which is sufficient to cross watersheds between river basins.

In full agreement with the previous studies of morphological variability of *M. petax*, this work also clearly confirms the similarity of the insular and mainland populations of the southern Far East (Maeda 1985; Yoshiyuki 1989; Tiunov 1997; Kruskop 2004; Gorobeyko et al. 2021), as well as the reliable differences between specimens from the Lake Khasan (Khasan group) and the rest of the Primorsky Territory sample (Tiunov 1997; Gorobeyko et al. 2021). The range of the Western Siberia morphological group coincides with the previously described distribution of the nominotypical subspecies (Kruskop 2004; Gorobeyko et al. 2021). The existence of a separate "Amurian morphological form" (Lower Amur group), similar to the Khasan group, is also supported (Gorobeyko et al. 2021). At the same time, we found that expanding the sample from the Middle Amur and Transbaikalia confirms the validity of the Baikal-Amur morphological group, which has not previously been proven in the studies (Kruskop 2004; Gorobeyko et al. 2021).

Unfortunately, it is not possible to genetically type all individuals whose morphological variability was analyzed, due to the fact that a large volume of museum material was used in the work. Furthermore, for many genotyped individuals, craniological material is not available. Nevertheless, the association between genetic lineages and morphological groups is partially present. We attempted to correlate the morphological groups identified during the morphometric analysis with previously described subspecies and genetic lineages discovered in this work (Fig. 6, Table 5).

(i) Specimens belonging to the Western Siberia morphological group and genetic lineage "Siberia" can be attributed to the nominotypical subspecies *M. p. petax*, described from the Chuya Steppe in the northwest of the Altai Mountains (Republic of Altai) (Hollister 1912).

(ii) Specimens with a combination of Baikal-Amur morphological group and genetic lineage "Amur" may be identified as *M. p. loukashkini*. The terra typica for the subspecies *M. p. loukashkini* is located in Wudalianchi City (Heilongjiang, China), and such a combination was found in the nearest localities, namely Lake Dolgoe (Amur Region) at a distance of 270 km and the Khalkhyn-Gol River (Mongolia) at a distance of 550 km. Moreover,

the craniological measurements of the holotype and paratype of *M. p. loukashkini* (Shamel 1942) fall within the limits of variability for the Baikal-Amur group. All this allows us to assume that a combination of the Baikal-Amur morphological group and genetic lineage "Amur" (ii) may be attributed to the subspecies *M. p. loukashkini*. A similar combination (ii) was also found in one individual from Tayshet City (Irkutsk Region).

(iii) Individuals with a combination of genetic lineage "Siberia" and Baikal-Amur morphological group may probably represent the result of hybridization between the *M. p. petax* (i) and *M. p. loukashkini* (ii).

(iv) Most individuals of *M. petax* from Primorsky Territory (with the exception of Lake Khasan) are characterized by a combination of the Far East morphological group and the genetic lineage "Siberia." It would be possible to assume that this combination may be inherent in the subspecies *M. p. ussuriensis* described from this territory. Nevertheless, in the putative range of *M. p. ussuriensis*, we also found combinations of the Far East morphological group with other genetic lineages.

(v) Specimens of *M. petax* belonging to the lineage "Okhotsk" and the Far East morphological group are distributed mainly on Sakhalin Island with isolated individuals in the south of Primorsky Territory. Presumably, this combination may be found in *M. petax* from adjacent areas of China (Jilin and Heilongjiang province).

(vi) Specimens of *M. petax* belonging to the lineage "Kunashir" and the Far East morphological group are found only on Kunashir Island. Previously, Maeda (1985) and Yoshiyuki (1989) did not find significant differences between *M. petax* from the Sakhalin Island, Kunashir Island, and Hokkaido Island, as well as from North Korea, and classified all of them as the subspecies *M. p. ussuriensis*.

(vii) The specimen from the Spasskaya Cave (Primorsky Territory) belongs to the lineage "Amur" and the Far East morphological group.

All this indicates the absence of a specific genetic lineage distinguishing the subspecies *M. p. ussuriensis*, in contrast to the condition observed in the nominotypical subspecies (i) and *M. p. loukashkini* (ii). Previously, a discrepancy in the distribution of two mitochondrial lineages and two morphological forms was revealed in *Eptesicus serotinus* Schreber, 1774 (Artyushin et al. 2009, 2012). The possible explanation for this may be incomplete lineage sorting, as well as introgression and fixation of alien mtDNA haplotypes.

(viii) Most of *M. petax* from Lower Amur (Khabarovsk Territory) are identified as the Lower Amur morphological group in combination with the genetic lineage "Okhotsk". Previously we designated these specimens as the "Amurian morphological form" (Gorobeyko et al. 2021).

(ix) The exception is one specimen with a combination of the Lower Amur group and the lineage "Siberia".

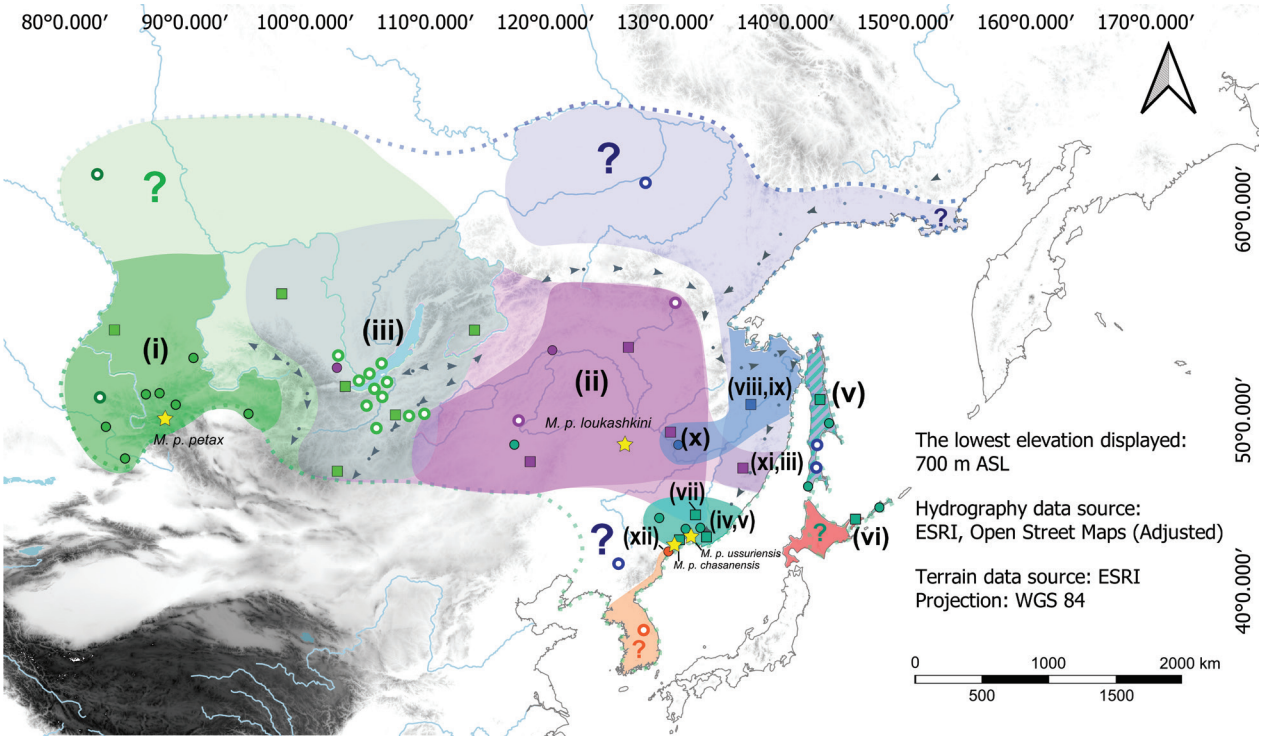

Figure 6. Ranges of genetic lineages and morphological groups. For Roman numerals, see text. Asterisks indicate the type locality for each subspecies. Empty circles and filled circles represent localities from which only genetic or morphological data were obtained, respectively. The colors of the circles correspond to Figures 3, 5. The squares indicate localities where both genetic and morphological data were studied. The colors of the squares correspond to the colors of the morphological groups. Gray arrow heads show main watersheds within the species' range.

Table 5. Belonging of samples from the collecting sites to genetic lineages and morphological groups. Genetic – sampling localities for molecular-genetic analysis, Morphology – sampling localities for craniometric analysis, N – number of samples. R – Russian Federation, C – China, M – Mongolia, SK – Republic of Korea, AO – Autonomous Okrug. AMF – Amurian morphological form, MPP – *M. p. petax*, MPL – *M. p. loukashkini*, FES – Far Eastern group + "Siberia" lineage, FEK – Far Eastern group + "Kunashir" lineage. Other abbreviations are explained in the text.

Region	Genetic				Morphological				Combinations and subspecies	
	Code	N	lineage		Code	N	group			
R: Khanty-Mansi AO	**1**	3	Siberia						**?**	
R: Novosibirsk Region	**2**	1	Siberia						**i**	*M. p. petax*
					NN	4	Western Siberia			
Kazakhstan					**KB**	3	Western Siberia		**?**	
					KM	1	Western Siberia			
R: Altai Territory	**3**	6	Siberia						**i**	*M. p. petax*
R: Altai Republic					**AK**	1	Western Siberia			
					AA	4	Western Siberia			
					AI	1	Western Siberia			
					AT	2	Western Siberia			
R: Republic of Khakassia					**KS**	1	Western Siberia			
R: Republic of Tyva					**TY**	11	Western Siberia		**?**	
R: Irkutsk Region	**4**	2|1	Siberia	Amur	**IT**	3	Baikal-Amur		**iii|ii**	MPP+MPL
M: Uvurkhangai aimag	**5**	4	Siberia		**MO**	5	Baikal-Amur		**iii**	MPP+MPL
R: Irkutsk Region	**6**	3	Siberia						**iii**	MPP+MPL
	7	3	Siberia		**IK**	3	Baikal-Amur			
					IO	1	Baikal-Amur			
	8	3	Siberia							
	9	4	Siberia							
	10	3	Siberia							
M: Selenge aimag	**11**	1	Siberia						**?**	
R: Republic of Buryatia	**12**	3	Siberia						**iii**	MPP+MPL
	13	4	Siberia							
	14	3	Siberia							
	15	1	Siberia							
	16	1	Siberia							
	17	3	Siberia							
	18	4	Siberia		**BK**	3	Baikal-Amur			
R: Transbaikal Territory	**19**	1	Siberia						**iii|ii**	MPP+MPL
	20	1|1	Siberia	Amur						
	21	2|1	Siberia	Amur						
	22	1	Siberia							
R: Republic of Buryatia	**23**	11	Siberia		**BD**	4	Baikal-Amur		**iii**	MPP+MPL
R: Transbaikal Territory	**24**	5	Amur						**ii**	*M. p. loukashkini*
C: Inner Mongolia					**CI**	2	Far East		**?**	
M: Dornod aimag	**25**	6	Amur		**MK**	7	Baikal-Amur		**ii**	*M. p. loukashkini*
R: Transbaikal Territory					**TS**	2	Baikal-Amur		**ii**	*M. p. loukashkini*
R: Sakha Republic	**26**	3	Okhotsk						**?**	
R: Amur Region	**27**	9	Amur		**ZE**	25	Baikal-Amur		**ii**	*M. p. loukashkini*
	28	2	Amur							
	29	10	Amur		**AR**	17|6	Baikal-Amur	Lower Amur	**ii|x**	MPL+AMF
					AG	1	Lower Amur		**x**	MPL+AMF
C: Heilongjiang					**CH**	2	Baikal-Amur		**?**	
R: Khabarovsk Territory	**30**	2	Okhotsk		**HT**	2	Lower Amur		**viii**	AMF
	31	1|9	Siberia	Okhotsk	**HG**	5	Lower Amur		**ix|viii**	MPL+ AMF+ FES
	32	1|3	Siberia	Okhotsk	**HP**	3	Baikal-Amur		**iii|xi**	

Region	Genetic				Morphological			Combinations and subspecies	
	Code	N	lineage		Code	N	group		
R: Primorsky Territory	**33**	1|1	Okhotsk	Amur	**PS**	2	Far East	**v|vii**	MPL+AMF+FES
	34	5	Siberia					**iv**	FES
	35	6|1	Siberia	Okhotsk	**PV**	8	Far East	**iv|v**	FES+AMF
					PU	2	Far East	**iv**	FES
					PP	6	Far East		
	36	1	Siberia		**PB**	1	Far East		
	37	2	Siberia		**PR**	2	Far East		
	38	10	Siberia		**PT**	10	Far East		
	39	4	Siberia		**PM**	4	Far East		
					PK	1	Far East		
					HA	17	Khasan	**xii**	*M. p. chasanensis*
	40	1|3	Siberia	Okhotsk				**iv|v**	FES+AMF
R: Sakhalin Island	**41**	1	Okhotsk					**v**	FES+AMF?
	42	2	Okhotsk						
	43	1	Okhotsk						
	44	2	Okhotsk						
					SK	4	Far East		
					SN	1	Far East		
					SP	1	Far East		
R: Iturup Island					**IP**	2	Far East	**?**	
R: Kunashir Island	**45**	1	Kunashir		**KA**	2	Far East	**vi**	FEK
	46	2	Kunashir		**KO**	2	Far East		
	47	3	Kunashir						
C: Jilin	**48**	1	Okhotsk					**?**	
SK: Gangwon Province	**49**	4	Korea					**?**	

"The Amurian morphological form" has essential differences from the other morphological groups and, moreover, cannot be related to any described subspecies. Greater similarity is observed with the Khasan group; however, the Lower Amur group is distinguished by larger average values of condylobasal and condylocanine length and width between the maxillary teeth. It can be assumed that the genetic lineage "Okhotsk" is inherent in the Lower Amur group, which, in turn, can serve as another argument confirming the validity of the "Amurian morphological form" as a form of subspecific rank. In this case, specimens with a combination of the lineage "Okhotsk" and the Far East group (v) or the lineage "Siberia" with the Lower Amur group (ix) may be hybrids of the "Amurian morphological form" (viii) and individuals combining the Far East group and the lineage "Siberia" (iv).

(x) Part of the Middle Amur sample (Amur Region) belongs to the Lower Amur morphological group and genetic lineage "Amur," while the other part of this sample is identified as *M. p. loukashkini* (ii).

(xi) Most specimens of *M. petax* from the Proschalnaya Cave (Khabarovsk Territory) belong to the genetic lineage "Okhotsk" and the Baikal-Amur morphological group.

These facts may indicate a possible contact zone between the "Amurian morphological form" (viii) and *M. p. loukashkini* (ii) at the border of their ranges.

(xii) Specimens of *M. petax* belonging to the Khasan group are found only near Lake Khasan, the southernmost part of the Primorsky Territory. These individuals are, on average, larger than the rest of the sample and were previously described as the subspecies *M. p. chasanensis* from Khasan District of the Primorsky Territory (Tiunov 1997). In certain publications, subspecies *M. p. chasanensis* was reduced to a synonym of *M. p. loukashkini* (Kruskop 2004). Nevertheless, the data obtained in the present work do not support such consolidation.

Unfortunately, due to the lack of material for genetic analysis, it was not possible to establish correspondence of the Khasan group to any genetic lineage. It is worth noting, however, that a distinct genetic lineage, "Korea," has been identified in the relatively nearby Gangwon Province of South Korea. According to morphometric data (Yoon et al. 2010), specimens from Gangwon, North Gyeongsang, Jeonbuk and Jeonnam provinces (South Korea), presumably belonging to this genetic lineage, are on average larger in craniometric parameters than other *M. petax* (Gorobeyko et al. 2021). On the contrary, *M. petax* from South Pyongan Province (North Korea) shows a high degree of similarity with the Japanese specimens in craniometric measurements (Maeda 1985). The relationship between *M. p. chasanensis* and genetic lineage "Korea" appears to still require further study.

Conclusion

For the first time, a detailed description of the intraspecific structure of *M. petax* has been presented using both morphological and molecular information. From our investigations, we discovered three common genetic lineages: "Okhotsk," "Amur," and "Siberia," and uncovered that the range of these genetic lineages seems to be connected to large river systems. Notably, "Korea" and "Kunashir," the two local and most genetically distinct lineages, are exclusive to the Korean Peninsula and Kunashir Island, respectively. The cohabitation of various genetic lineages has been established only for territories where different river basins are connected, such as the Primorsky Territory, Khabarovsk Territory, Transbaikalia Territory, and Mongolia.

We revealed the five morphological groups, which only partially correlated with genetic lineages and morphological subspecies. The two subspecies previously described for *M. petax* sensu stricto can apparently be defined as a specific combination of a morphological group with a genetic lineage. Thus, *M. p. petax* can be characterized as specimens belonging to the Western Siberia morphological group and genetic lineage "Siberia," while *M. p. loukashkini* represents a combination of the Baikal-Amur morphological group with the genetic lineage "Amur." Accordingly, a distinctive feature of *M. p. loukashkini* is the presence of additional R1 repeats in the control region of mtDNA, found only in the lineage "Amur."

The subspecies structure of *M. petax* in the southern Far East remains unclear and still requires further study. We found the absence of a specific genetic lineage distinguishing the individuals in the putative range of *M. p. ussuriensis*, in contrast to the condition observed in the nominotypical subspecies and *M. p. loukashkini*. On the contrary, the lack of genetic data from the type locality does not allow establishing the relation of *M. p. chasanensis* with any genetic lineage.

Most specimens of the "Amurian morphological form" are characterized by a specific combination of the Lower Amur morphological group and the genetic lineage "Okhotsk," which may possibly serve as confirmation of the validity of "Amurian morphological form" as a form of subspecific rank.

Acknowledgements

We are especially grateful to the members of Vladivostok Caving Club for the organization of field works in the caves of Primorsky Territory. We would like to thank Dr. Oleg N. Morozov (Center of Children's Complementary Education and Evenkis' Folk Crafts, Bagdarin, Russia), Yulia A. Mel'nikova and Denis N. Kochetkov (Khingan Nature Reserve), Sergey Yu. Ignatenko and Elena V. Ignatenko (Zeya Nature Reserve), Dr. Alexander D. Botvinkin (Irkutsk State Medical University, Irkutsk, Russia), Dr. Maxim A. Khasnatinov (Federal State Public Science Institution "Scientific Centre for Family Health and Human Reproduction Problems," Irkutsk, Russia), Vladimir S. Lebedev and Yaroslav A. Red'kin (Zoological Museum of the Lomonosov Moscow State University, as well as part of Joint Russian-Mongolian Complex Biological Expedition of the Russian Academy of Sciences and Mongolian Academy of Sciences), Alexandra P. Shumkina, Elena Yu. Shumkina, Alexander B. Alekseev and Evgeny Raspopov ("Mechta," Irkutsk, Russia), Nikolai V. Yakovchic (Irkutsk, Russia), Vadim V. Bobrovsky and Polina S. Van (Petrenko) (Komsomolsk-on-Amur, Russia), Evgeny E. Kozlovsky (Yuzhno-Kurilsk, Russia), Vasily V. Gorobeyko (Vladivostok, Russia) for their help in mounting the expeditions. We express our sincere gratitude to the reviewers for their adequate assessment of the manuscript and valuable comments that allowed us to improve the manuscript. We sincerely thank Haneef Ahmed Amissah, a native English speaker, who corrected language errors in the article.

The research was carried out within the state assignment of Ministry of Science and Higher Education of the Russian Federation theme No. 124012200182-1 (Federal Scientific Center of the East Asia Terrestrial Biodiversity of FEB RAS), theme No. 121030900138-8 (Institute of General and Experimental Biology of SB RAS), and state theme of scientific work of the ZMMU No. 121032300105-0.

References

Aljanabi S, Martinez I (1997) Universal and rapid salt-extraction of high quality genomic DNA for PCR-based techniques. Nucleic Acids Research 25: 4692–4693. https://doi.org/10.1093/nar/25.22.4692

Artyushin IV, Bannikova AA, Lebedev VS, Kruskop SV (2009) Mitochondrial DNA relationships among North Palaearctic *Eptesicus* (Vespertilionidae, Chiroptera) and past hybridization between common serotine and northern bat. Zootaxa 2262: 40–52. https://doi.org/10.11646/zootaxa.2262.1.2

Artyushin IV, Lebedev VS, Smirnov DG, Kruskop SV (2012) Taxonomic position of the Bobrinski's serotine (*Eptesicus bobrinskoi*, Vespertilionidae, Chiroptera). Acta Chiropterologica 14: 291–303. https://doi.org/10.3161/150811012X661620

Берников КА; Крускоп СВ; Стариков ВП [Bernikov KA, Kruskop SV, Starikov VP] (2011) Восточная ночница (*Myotis petax* Hollister, 1912) – новый вид рукокрылых Ханты–Мансийского автономного округа. [Eastern water bat (*Myotis petax* Hollister, 1912) – New bat species of Khanty-Mansiy autonomous okrug.] In: Стариков ВП [Starikov VP] (Ed.) Материалы Всероссийской научной конференции; посвящённой 15-летию биологического факультета Сургутского государственного университета, Сургут, 2–4 июня 2011 г. Таймер, Сургут, 45–49.

Bogdanowicz W (1994) *Myotis daubentonii*. Mammalian Species 475: 1–9. https://doi.org/10.2307/3504215

Ботвинкин АД [Botvinkin AD] (2002) Летучие мыши в Прибайкалье (биология; методы наблюдения; охрана). [Bats in Baikal region (natural history, observation methods, conservation).] Время странствий, Иркутск, 208 pp.

Bouckaert R, Vaughan TG, Barido-Sottani J, Duchêne S, Fourment M, Gavryushkina A, Heled J, Jones G, Kühnert D, De Maio N, Matschiner

M, Mendes FK, Müller NF, Ogilvie HA, du Plessis L, Popinga A, Rambaut A, Rasmussen D, Siveroni I, Suchard MA, Wu CH, Xie D, Zhang C, Stadler T, Drummond AJ (2019) BEAST 2.5: An advanced software platform for Bayesian evolutionary analysis. PLoS Computational Biology 15: e1006650. https://doi.org/10.1371/journal.pcbi.1006650

Didorenko SI, Botvinkin AD, Takhteev VV (2022) *Myotis petax* (Chiroptera, Vespertilionidae) preys on pelagic Amphipoda (Crustacea, Gammaroidea) of Lake Baikal. Acta Chiropterologica 24: 187–194. https://doi.org/10.3161/15081109ACC2022.24.1.015

Excoffier L, Lischer HE (2010) Arlequin suite ver 3.5: A new series of programs to perform population genetics analyses under Linux and Windows. Molecular Ecology Resources 10: 564–567. https://doi.org/10.1111/j.1755-0998.2010.02847.x

Гениатулин РФ [Geniatulin RF] (2009) Малая энциклопедия Забайкалья: Природное наследие. [Small encyclopedia of Transbaikalia: Natural heritage.] Наука, Новосибирск, 698 pp.

Gorobeyko UV, Kartavtseva IV, Sheremetyeva IN, Kazakov DV, Guskov VY (2020) DNA-barcoding and a new data about the karyotype of *Myotis petax* (Chiroptera, Vespertilionidae) in the Russian Far East. Comparative Cytogenetics 14: 483–500. https://doi.org/10.3897/CompCytogen.v14i4.54955

Горобейко УВ, Шереметьева ИН, Казаков ДВ [Gorobeyko UV, Scheremetyeva IN, Kazakov DV] (2021) Краниометрическая изменчивость восточной ночницы *Myotis petax* Hollister, 1912 (Vespertilionidae, Chiroptera) на юге Дальнего Востока России. [Craniological variability of Eastern water bat *Myotis petax* Hollister, 1912 (Vespertilionidae, Chiroptera) on the Southern Russian Far East.] Биота и среда природных территорий 3: 71–87. https://doi.org/10.37102/2782-1978_2021_3_5

Gorobeyko UV, Sheremetyeva IN, Kazakov DV, Guskov VY (2023) A new type of tandem repeats in *Myotis petax* (Chiroptera, Vespertilionidae) mitochondrial control region. Molecular Biology Reports 50: 5137–5146. https://doi.org/10.1007/s11033-023-08468-4

Громов ИМ, Гуреев АА, Новиков ГА, Соколов ИИ, Стрелков ПП, Чапский КК [Gromov IM, Gureev AA, Novikov GA, Sokolov II, Strelkov PP, Chapskij KK] (1963) Млекопитающие фауны СССР. Ч. 1. [Mammals of the fauna of the USSR. P. 1.] In: Соколов ИИ [Sokolov II] (Ed.) Определители по фауне СССР, издаваемые Зоологическим институтом АН СССР 82: 1–640.

Hao X (2019) Complete mitochondrial genome of the East Asian fish-eating bat: *Myotis ricketti* (Chiroptera, Vespertilionidae). Mitochondrial DNA Part B 4: 3748–3749. https://doi.org/10.1080/23802359.2019.1681316

Hollister N (1912) New mammals from the highlands of Siberia. Smithsonian Miscellaneous Collection 60: 1–6. https://doi.org/10.5962/bhl.part.7637

Hutterer R, Ivanova T, Meyer-Cords C, Rodrigues L (2005) Bat migrations in Europe: A review of literature and analysis of banding data. Naturschutz und Biologische Vielfalt 28: 1–172.

Hwang JY, Jin GD, Park J, Lee SG, Kim EB (2016) Complete sequences of eastern water bat, *Myotis petax* (Chiroptera; Microchiroptera; Vespertilionidae) mitogenome. Mitochondrial DNA Part A 27: 3715–3716. https://doi.org/10.3109/19401736.2015.1079871

Jo YS, Baccus JT, Koprowski JL (2018) Mammals of Korea: A review of their taxonomy, distribution and conservation status. Zootaxa 4522: 1–216. https://doi.org/10.11646/zootaxa.4522.1.1

Kalyaanamoorthy S, Minh BQ, Wong TKF, von Haeseler A, Jermiin LS (2017) ModelFinder: Fast model selection for accurate phylogenetic estimates. Nature Methods 14: 587–589. https://doi.org/10.1038/nmeth.4285

Kawai K (2015) *Myotis petax*. In: Ohdachi SD, Ishibashi Y, Iwasa MA, Fukui D, Saitoh T (Eds) The Wild Mammals of Japan, 2nd Ed. Shoukadon Book Sellers, Kyoto, 112–113.

Kazakov DV, Artyushin IV, Khabilov TK, Tadzhibaeva DE, Kruskop SV (2020) Back to life and to taxonomy: New record and reassessment of *Myotis bucharensis* (Chiroptera: Vespertilionidae). Zootaxa 4878: 129–144. https://doi.org/10.11646/zootaxa.4878.1.5

Koopman KF (1994) Chiroptera: Systematics. In: Niethammer J, Schliemann H, Stark D (Eds) Handbook of Zoology. Vol. VIII Mammalia, Part 60. Walter de Gruyter, Berlin, 1–217. https://doi.org/10.1515/9783110888157

Kruskop SV (2004) Subspecific structure of *Myotis daubentonii* (Chiroptera, Vespertilionidae) and composition of the "*daubentonii*" species group. Mammalia 68: 299–306. https://doi.org/10.1515/mamm.2004.029

Kruskop SV, Borisenko AV, Ivanova NV, Lim BK, Eger JL (2012) Genetic diversity of northeastern Palaearctic bats as revealed by DNA barcodes. Acta Chiropterologica 14: 1–14. https://doi.org/10.3161/150811012X654222

Кузякин АП [Kuzyakin AP] (1950) Летучие мыши. [Bats.] Советская наука, Москва, 443 pp.

Link W, Dixkens C, Singh M, Schwall M, Melchinger AE (1995) Genetic diversity in European and Mediterranean faba bean germ plasm revealed by RAPD markers. Theoretical and Applied Genetics 90: 27–32. https://doi.org/10.1007/BF00220992

Lu G, Lin A, Luo J, Blondel DV, Meiklejohn KA, Sun K, Feng J (2013) Phylogeography of the Rickett's big-footed bat, *Myotis pilosus* (Chiroptera: Vespertilionidae): A novel pattern of genetic structure of bats in China. BMC Evolutionary Biology 13: 241. https://doi.org/10.1186/1471-2148-13-241

Maeda K (1985) New Records of the eastern Daubenton's bats, *Myotis daubentoni ussuriensis* Ognev, 1927, in Hokkaido and variations in external and skull dimensions. Journal of the Mammalogical Society of Japan 10: 159–164.

Matveev VA, Kruskop SV, Kramerov DA (2005) Revalidation of *Myotis petax* Hollister, 1912 and its new status in connection with *M. daubentonii* (Kuhl, 1817) (Vespertilionidae, Chiroptera). Acta Chiropterologica 7: 23–37. https://doi.org/10.3161/1733-5329(2005)7[23:ROMPHA]2.0.CO;2

Матюшкин ЕН [Matyushkin EN] (1976) Европейско-восточноазиатский разрыв ареалов наземных позвоночных. [European-East-Asian break between the ranges of terrestrial vertebrates.] Зоологический журнал 55: 1277–1291.

Матюшкин ЕН [Matyushkin EN] (1982) Региональная дифференциация лесной фауны Палеарктики в прошлом и настоящем. [Regional differentiation of Palaearctic forest fauna in past and present.] In: Дроздов НН, Максимова ВФ, Мяло ЕГ, Соколов ИА [Drozdov NN, Maksimova VF, Myalo EG, Sokolov IA] (Eds) Теоретические и прикладные аспекты биогеографии. Наука, Москва, 59–80.

Nguyen LT, Schmidt HA, von Haeseler A, Minh BQ (2015) IQ-TREE: A fast and effective stochastic algorithm for estimating maximum likelihood phylogenies. Molecular Biology and Evolution 32: 268–274. https://doi.org/10.1093/molbev/msu300

Огнёв СВ [Ognev SV] (1928) Звери Восточной Европы и Северной Азии. Т. 1. [Mammals of Eastern Europe and Northern Asia. Vol. 1.] Госиздат, Москва, Ленинград, 631 pp.

Rozas J, Ferrer-Mata A, Sánchez-DelBarrio JC, Guirao-Rico S, Librado P, Ramos-Onsins SE, Sánchez-Gracia A (2017) DnaSP 6: DNA Sequence polymorphism analysis of large datasets. Molecular Biology and Evolution 34: 3299–3302. https://doi.org/10.1093/molbev/msx248

Scheffler I, Jargalsaikhan A, Bolorchimeg I, Stubbe A, Stubbe M, Abraham A, Thiele KD (2016) Bat ectoparasites of Mongolia, part 3. Exploration into the Biological Resources of Mongolia 13: 395–408.

Schmitz A, Riesner D (2006) Purification of nucleic acids by selective precipitation with polyethylene glycol 6000. Analytical Biochemistry 354: 311–313. https://doi.org/10.1016/j.ab.2006.03.014

Shamel HH (1942) A new *Myotis* from Manchuria. Proceedings of the Biological Society of Washington 55: 103–104.

Sievers F, Wilm A, Dineen DG, Gibson TJ, Karplus K, Li W, Lopez R, McWilliam H, Remmert M, Söding J, Thompson JD, Higgins DG (2011) Fast, scalable generation of high-quality protein multiple sequence alignments using Clustal Omega. Molecular Systems Biology 7: 539. https://doi.org/10.1038/msb.2011.75

Smith AT, Xie Y, Hoffmann RS, Lunde D, MacKinnon J, Wilson DE, Wozencraft WC (2008) A guide to the mammals of China. Princeton University Press, Princeton, NJ, 576 pp.

Tamura K, Nei M (1993) Estimation of the number of nucleotide substitutions in the control region of mitochondrial DNA in humans and chimpanzees. Molecular Biology and Evolution 10: 512–526. https://doi.org/10.1093/oxfordjournals.molbev.a040023

Тиунов МП [Tiunov MP] (1984) Отряд Рукокрылые – Летучие мыши. [Order Chiroptera Blumenbach, 1779 – Bats.] In: Кривошеев ВГ [Krivosheev VG] (Ed.) Наземные млекопитающие Дальнего Востока СССР. Наука, Москва, 73–102.

Тиунов МП [Tiunov MP] (1985) Зимующие рукокрылые (Chiroptera) юга Дальнего Востока СССР. [Wintering Chiroptera in the south of the Far East.] Зоологический журнал 64: 1595–1599.

Тиунов МП [Tiunov MP] (1997) Рукокрылые Дальнего Востока России. [Bats of the Russian Far East.] Дальнаука, Владивосток, 134 pp.

Tiunov MP, Makarikova TA (2007) Seasonal molting in *Myotis petax* (Chiroptera) in the Russian Far East. Acta Chiropterologica 9: 538–541. https://doi.org/10.3161/1733-5329(2007)9[538:SMIMPC]2.0.CO;2

Wang L, Jiang TL, Sun KP, Wang YX, Tiunov MP, Feng J (2010) Morphological description and taxonomical status of *Myotis petax*. Acta Zootaxonomica Sinica 35: 360–365.

Wu Z, Han Y, Wang Y, Liu B, Zhao L, Zhang J, Su H, Zhao W, Liu L, Bai S, Dong J, Sun L, Zhu Y, Zhou S, Song Y, Sui H, Yang J, Wang J, Zhang S, Qian Z, Jin Q (2022) A comprehensive survey of bat sarbecoviruses across China in relation to the origins of SARS-CoV and SARS-CoV-2. National Science Review 10: nwac213. https://doi.org/10.1093/nsr/nwac213

Yoon MH (2010) Vertebrate Fauna of Korea, vol. 5, no. 1, Bats. National Institute of Biological Resources, Incheon, 134 pp.

Yoshiyuki MA (1989) Systematic study of the Japanese Chiroptera. National Science Museum, Tokyo, 242 pp.

Zhigalin AV, Khritankov AM (2014) Bats of SPNAs of the Altai-Sayan mountain country. Plecotus et al. 17: 85–95.

Supplementary Material 1

File S1

Authors: Uliana V. Gorobeyko, Denis V. Kazakov, Anastasia A. Kadetova, Irina N. Sheremetyeva, Valentin Yu. Guskov, Irina V. Kartavtseva, Nikolai E. Dokuchaev, Evgeniy S. Zakharov, Sergei V. Kruskop

Data type: .xlsx

Explanation notes: tables S1–S4.

Link: https://doi.org/10.3897/vz.74.e128528.suppl1

Supplementary Material 2

File S2

Authors: Uliana V. Gorobeyko, Denis V. Kazakov, Anastasia A. Kadetova, Irina N. Sheremetyeva, Valentin Yu. Guskov, Irina V. Kartavtseva, Nikolai E. Dokuchaev, Evgeniy S. Zakharov, Sergei V. Kruskop

Data type: .png

Explanation notes: Craniodental measurements of *Myotis* bat skull.

Link: https://doi.org/10.3897/vz.74.e128528.suppl2

Supplementary Material 3

File S3

Authors: Uliana V. Gorobeyko, Denis V. Kazakov, Anastasia A. Kadetova, Irina N. Sheremetyeva, Valentin Yu. Guskov, Irina V. Kartavtseva, Nikolai E. Dokuchaev, Evgeniy S. Zakharov, Sergei V. Kruskop

Data type: .docx

Explanation notes: Tandem repeats and sequence length variability.

Link: https://doi.org/10.3897/vz.74.e128528.suppl3